

Bone Micro-Fracture Observations From Direct Impact of Slow Velocity Projectiles

David Christopher Kieser^{1,*}, Riley Riddell¹, Julius August Kieser², Jean-Claude Theis², Michael Vernon Swain²

¹Department of Surgical Sciences, Dunedin School of Medicine, Division of Health Sciences, University of Otago, Dunedin, New Zealand

²Sir John Walsh Research Institute, University of Otago, Dunedin, New Zealand

*Corresponding author: David Christopher Kieser, P.O.Box: 6458, Dunedin, 9016, New Zealand. Tel: +64-211499829, Fax: +64-034679709, E-mail: kieser david@gmail.com.

Received: October 25, 2013; **Revised:** November 10, 2013; **Accepted:** November 19, 2013

Background: Skeletal fractures produced by bullet impacts are unique and yet their mechanism remains poorly understood.

Objectives: To understand the initiation and propagation of direct ballistic skeletal fractures on cylindrical bones.

Materials and Methods: We observed the effect of 9 mm spherical non-deforming steel projectiles fired at increasing velocities of 10 ft/s (3 m/s) to 200 ft/s (60 m/s) (pre-impact kinetic energy of 0.013-5.35 J) directly upon skeletally mature deer femora. Skeletal damage was assessed following micro-computed tomography and fluorescent microscopy.

Results: A cascade of injury severity was identified, with fractures first seen at a pre-impact kinetic energy of 1.08 J and progressing from localized micro-fragmentation and indentation to long radiating fractures. Bone indentation was found to increase with increasing projectile speed.

Conclusions: The deformation and resultant fracture process occurs as a reproducible cone crack cascade with an expanding zone of fragmentation. This knowledge should aid clinicians in understanding the formation of fracture fragments, the forces exerted on these fragments and the areas of residual weakness to ensure optimal skeletal management.

Keywords: Forensic Ballistics; Fractures, Bone; Wounds, Gunshot; Orthopedics

1. Background

Skeletal fracture occurs in almost half of all patients admitted for civilian gunshot wounds (1). These fractures are unique; however, the mechanisms responsible for the resultant damage are poorly understood. It is clear that the high kinetic energy of gunshot projectiles potentiate a large force, over a small area at a high rate (2). It has been proposed that the rate of energy transfer is too high for visco-elastic compensation and therefore, the bone behaves as a brittle material under these circumstances (3). The resultant bone fractures produced therefore tend to be highly comminuted and extensive. Previous studies have macroscopically observed the patterns of fracture seen in direct projectile injuries producing gross fracture (4-6). From these observations, theories as to the mechanism of how bone fractures in direct ballistic trauma have been proposed. Despite its obvious clinical and forensic importance, little attention has been paid to the biomechanical nature of such injuries. A number of recent studies have produced biomechanical insights into ballistic fracture patterns in pig mandibles (7, 8) but there are still no data on similar patterns in round bones.

Recently, Wrightman et al. demonstrated the potential usefulness of using micro-CT to investigate the behavior of air rifle pellets in ballistic gel and their interaction with bone (9). However, their study focused mainly on the penetration of pellets into a gel medium and their subsequent deformation, rather than their effect on bone. The aim of this study was to understand how the fractures develop and propagate in direct ballistic skeletal injury to cylindrical bones.

2. Objectives

The objectives of this research were to develop an understanding of the behavior of a cylindrical bone during low velocity impact by studying the patterns of fracture initiation and propagation of such injuries, and to describe the fracture cascade that occurs in ballistic skeletal trauma.

3. Materials and Methods

We observed the effect of 9 mm (2.9735 g) spherical non-deforming steel projectiles fired between 10 ft/s (3 m/s) and 200 ft/s (60 m/s) (pre-impact kinetic energy of 0.013-5.35 J) directly upon the anterior mid-shaft of 21

Implication for health policy/practice/research/medical education:

This research has implications for health practitioners, in particular orthopedic surgeons, for understanding how fractures develop and therefore the best way of managing the injury.

Copyright © 2014, Aja University of Medical Sciences; Published by Kowsar Corp. This is an open-access article distributed under the terms of the Creative Commons Attribution License, which permits unrestricted use, distribution, and reproduction in any medium, provided the original work is properly cited.

skeletally mature female red deer (*Cervus elaphus*) rear femora. Deer femora were used because of their morphological and biomechanical similarity to human femora (10). The samples were obtained from a local processing plant within 4 hours of slaughter, maintained at 4°C wrapped in isotonic saline soaked gauze and stripped of soft tissue, but, preserving the periosteum, until testing at room temperature. The projectiles were fired at the bones, which were rigidly clamped at either end, using an Argon pneumatic ballistic device (Figure 1) similar to the Helium gas gun described by Huelke et al. (11, 12).

After macroscopic examination of the injury, a 50 mm portion of the mid-diaphysis was excised around the impact zone. Ten of the femora were then scanned with a SkyScan 1172 high-resolution micro-CT (Kontich, Belgium) at a resolution of 17 µm/pixel, processed with Nrecon reconstruction software and viewed with image J as a stack. Orthogonal and 3D views were used in the analysis of the image stacks. Two control specimens of non-impacted femora were used for comparison. A further 10 samples were stained en bloc with basic fuchsin after injury, using the procedure outlined by Burr et al. and compared with 2 identical samples without injury (13). These samples were sectioned into 500 µm thick coronal sections, with an accutom precision cut-off machine (Struers, Ballerup, Denmark). The sections were mounted on a glass slide with PermaBond 910 adhesive, and ground to symmetrical samples of 150 µm thickness with a modular preparation system (LaboSystem, Struers, Ballerup, Denmark). The samples were analyzed under light and fluorescent microscopy (545 nm wavelength).

A final sample was sawn at each end of the shaft and the marrow removed, prior to being shot at 155 ft/s (47 m/s, 3.28 J). This sample was observed macroscopically and under micro-CT, and then compared with the previous whole bone samples shot at a similar velocity. This sample was used to assess the role of the bone marrow in such injuries.

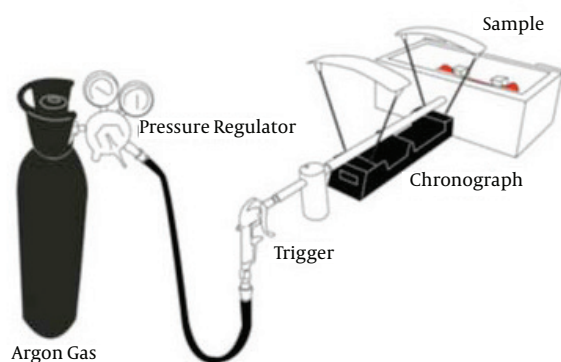


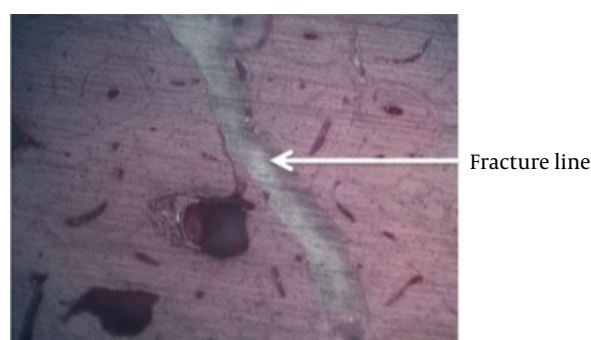
Figure 1. Argon Ballistic Gas Gun Device Used to Fire 9 mm Spherical Projectiles at Variable Velocities

4. Results

The 2 control specimens analyzed under micro-CT did not appear to have any fractures; however, in the control specimens stained with basic fuchsin, micro-cracks were seen resulting from the preparatory process (Figure 2). These cracks were difficult to differentiate from those incurred during impact and therefore, this method of analysis was abandoned due to its poor reliability in differentiating damage caused by the injury rather than the preparatory process.

Under micro-CT analysis no evidence of injury was seen at impacts below 40 ft/s (12 m/s, 0.21 J). Between 40 ft/s (12 m/s, 0.21 J) and 90 ft/s (27 m/s, 1.08 J) permanent indentation and bone impaction without underlying fracture was seen (Figure 3). This indentation induced deformation increased with impact velocity (Figure 4).

Figure 2. A Microscopic View of a Fractures Within the Compact Bone, Stained En Bloc With Basic Fuchsin



A fracture from the impact is difficult to delineate from one produced during the preparatory process.

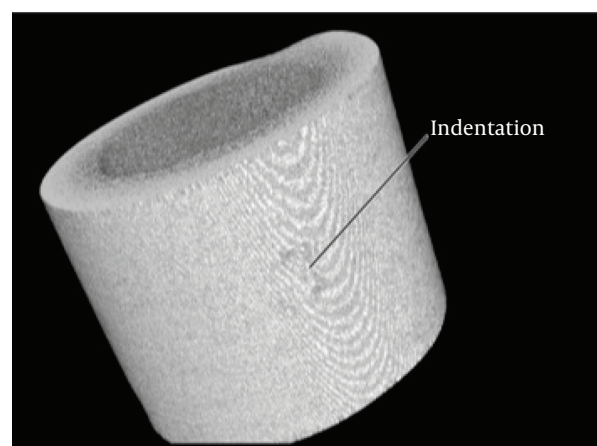


Figure 3. Micro-CT of the Impact Site of a Deer Femur Shot at 75 ft/s (23 m/s), Showing Cortical Indentation Without Fracture

The threshold for fracture was found to be a pre-impact kinetic energy of 1.08 J (90 ft/s, 27 m/s), where a single longitudinal crack in the sagittal plane was observed on the same side as the projectile's impact, initiating at the edge of the contact area. The micro-CT images show these are similar to a cone crack typically seen in brittle materials below spherical impact sites (14). A matching split in the periosteum over the impact site was also seen. At a pre-impact energy of 1.34 J (100 ft/s, 30 m/s) the beginnings of long radiating cracks in the form of a "double butterfly" became apparent. These fractures initiated almost parallel to the axis of the bone then extended at approximately 45° to the long axis of the bone. With increasing velocities, an expanding zone of fracture travelling through the bone away from the impact site at 90° to the projectile's direction, was also identified (Figure 5).

Above 1.62 J (110 ft/s, 33 m/s), the long radiating fractures were seen to extend to the opposite side of the bone, ultimately connecting with each other to form a longitudinal fracture on the far cortex to the impact site. Interestingly,

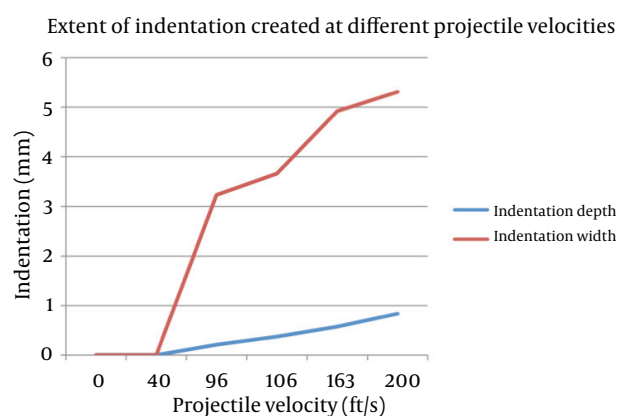


Figure 4. Indentation Depth and Width in Relation to Projectile Velocity

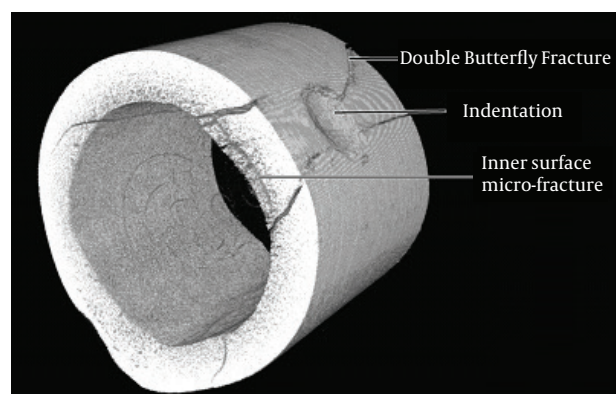


Figure 5. Micro-CT Image of the Impact Site of a Deer Femur Shot at 165 ft/s (50 m/s), Showing a Crack at the Edge of the Resultant Indentation, the Double Butterfly and Inner Surface Micro-Damage Fractures

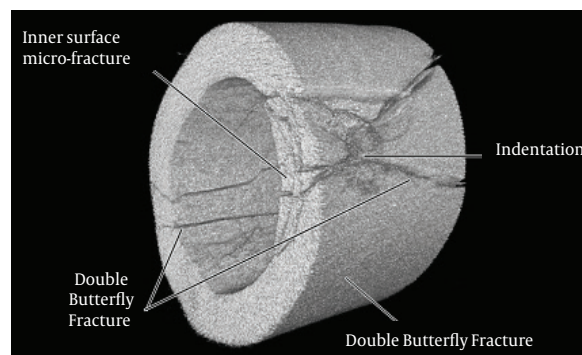


Figure 6. Micro-CT Image of the Impact Site of a Deer Femur Shot at 180 ft/s (54.5 m/s), Showing Deeper and More Extensive Indentation Damage, the Double Butterfly Fractures Extending Onto the Far Cortex Towards One Another and Progression of the Shockwave Comminution

these fractures did not appear to preferentially fracture through the intrinsic canals of the cortical bone. As the projectile speed was increased, the severity of the fracture worsened, with greater fracture width, indentation and comminution, but the fracture pattern remained unchanged (Figure 6). The sample with the marrow removed fractured with the same fracture pattern and equivocal extent as those seen in the whole bone samples impacted with the same velocity projectile.

5. Discussion

Understanding how bone breaks and analysing fracture patterns are important principals of orthopedics because it alludes the clinician to the areas of maximal trauma and associated injuries as well as allowing the clinician to predict the areas of residual weakness which determines the optimal management of the fracture.

Ballistic fractures are relatively common injuries with unique fracture patterns, but the mechanism of their formation remains unknown. Previous studies have focused on analyzing the fractures sustained from higher velocity projectile injuries (minimum velocity 200 ft/s) to theorize how fractures develop in direct ballistic injuries (4-6). However, this approach involves analyzing the patterns of complete and often comminuted fractures to predict how the fracture started, rather than analyzing slower range velocities to include the critical range of injuries from no permanent skeletal injury to complete fracture. To our knowledge, this is the first study utilizing this slower range of projectile velocities (10-200 ft/s) to analyze the initiation and propagation of direct ballistic fractures.

This study employed a reductionist approach to this complex injury by using slow-velocity, spherical, non-deforming, steel projectiles to analyze the initiation and propagation of ballistic fractures. This was to limit the number of variables, particularly projectile deformation, and reproduce impact surface areas with multiple sam-

ples. The resultant fractures show constant repeatability between sample groups and samples impacted at similar pre-impact velocities (Table 1). The fractures produced in this experiment were consistent with those previously reported in higher velocity injuries (4-6) and therefore, the extrapolation of these observations to higher velocity projectiles may help to explain the mechanism of injury in ballistic fractures.

There appears to be a critical impact kinetic energy required to initiate fracture of bone with the 9 mm diameter steel projectile used. At very low kinetic energies (< 0.21 J), the projectile may temporarily indent the cortex, however, this study design can only assess the permanent damage rather than dynamic changes in the bone. The presence of the thin soft periosteum may well have cushioned the initial impact minimizing the formation of permanent deformation. As the pre-impact energy increases (0.21-1.08 J) the periosteum is observed as having been cut and the bone is progressively indented and permanently compressed, but not fractured. This indentation depth increases with increased projectile velocity.

Beyond a critical energy a fracture cascade is initiated. The rather coarse pixel size (17 μm) of the micro-CT limits the resolution with which the 3D pattern of the fracture events can be clearly resolved. For impact kinetic energy of 1.08 J the micro-CT images show the presence of a cone-like crack that initiates at the edge of the contact area and extends into the bone. The extent of this is more evident parallel to the axis of the bone. With increasing pre-impact energy, the depth of the residual impression and the extent of the radial cracks become more readily evident. The crack is more readily seen as it is more open than many of the other cracks. This occurs because the plastic deformation associated with the permanent impression generated by the impact is now wedging open the cracks. Initially a small longitudinal fracture occurs

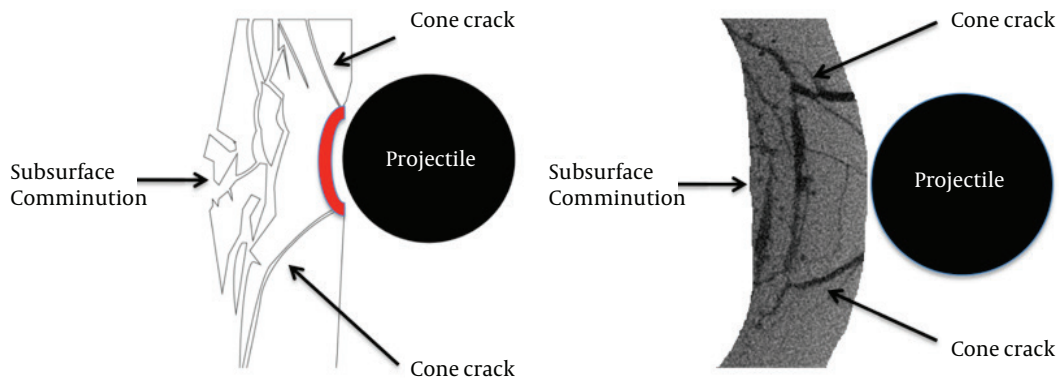
(1.08 J) and then enlarges with increasing velocity to form part of the classic double butterfly fracture (1.34 J). These fractures initiate from the impact site and are almost parallel to the bone axis before extending at approximately 45° to the long axis of the bone. Prior to these fractures extending as far as the opposite side to the bone fracture develops beneath the impact site oriented at 90° to the projectile trajectory. At the contact site there are multiple cone cracks that develop, as observed by Knight et al. (14) for glass, as well as axial cracks initiating from the internal surface of the bone as it is pressed into the subsurface cavity space. This combination of cone and axial cracks results in the comminution of the underlying bone at the point of impact (Figure 7).

With increased energy the superior and inferior butterfly fractures of each side extend to the opposite side of the bone (1.72 J), ultimately coming in contact with one another to form a longitudinal fracture on the opposite cortex, completing the double butterfly fracture pattern.

The first evidence of periosteal damage in our study was a longitudinal split mirroring the underlying longitudinal fracture. This occurred at the same critical energy required for fracture formation (1.08 J). With increased kinetic energy the periosteum was seen to progress from a single split to a stellate tear. It is likely however, that periosteal bruising will be seen below the threshold velocity for fracture, but our model of non-living, non-perfused tissue prevents such observations.

This proposed cascade of fracture initiation and propagation is consistent with observations of fracture events of brittle materials (14, 15). In both the latter studies the extent of the cracking and comminution increased with pre-impact energy. These observations are also the precursors to the observations suggested by Harger et al. who proposed, that as the projectile penetrates the bone it expands the wound tract at high velocity, forming 'shock

Figure 7. The Cone Crack (Arrowed) Fracture Pattern and Additional Subsurface Comminution as Observed Beneath the Impact site at Impact Velocities Slightly Above the Threshold for Crack Initiation



The red zone is the plastic or permanently deformed bone beneath the impact site.

Table 1. Summary of the Relationship Between Pre-impact Kinetic Energy and the Resultant Bone and Periosteal Injury

Preimpact Kinetic Energy, J	Effect	
	Bone	Periosteum
< 0.21	Non-permanent injury	Non-permanent injury
0.21-1.08	Indentation	Linear split
1.08-1.34	Longitudinal split	Stellate tear
1.34-1.72	Double butterfly and cone crack initiates	Progressive enlargement of stellate tear
> 1.72	Fractures extend to opposite side of bone	Progressive enlargement of stellate tear

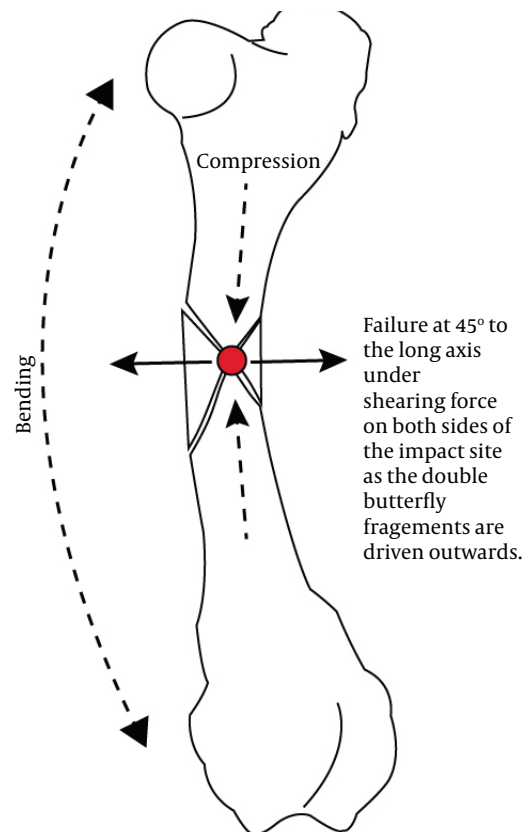
waves' which magnify the damage far beyond the simple drilling effect (16). We do suggest that in the current study, the role of shock waves is minimal and rather the expanding plug of bone that is displaced and extensively comminuted is a result of multiple cone cracks and the radial and vertical displacement of the bone beneath the impact site. Additionally, the fractures seen closely mirror those observed in higher velocity projectile injuries (4-6).

Previous reports have suggested that a forced flexion occurs on the opposite side to impact when the projectile impacts the bone, resulting in indirect failure from tension forces on that side of the bone (4) (Figure 8). Accepting that bone is weaker in tension than compression, one would therefore expect to see a transverse fracture pattern commencing on the opposite side to impact (4). In this study, no such fracture was identified. We therefore believe that the projectile itself does not deform the bone sufficiently for tension fracture on the opposite side of the bone to occur, unless it occurs by retardation of the temporary cavity in higher velocity injuries.

Similarly, as the sample without bone marrow fractured in a similar fashion to the whole bone samples, we believe it unlikely that pressure within the marrow cavity is responsible for the formation of the observed fracture patterns. This contrasts with the view of Sellier et al. who discusses increased intra-medullary pressure as a mechanism for ballistic fracture (17).

As this study examined only low velocity projectiles, it is limited in its ability to assess the effect of the temporary cavity and violence of higher velocity injuries, which may impart different forces on the bone (17). However, due to the remarkable similarity between the fracture patterns seen in high velocity ballistic trauma and those observed in this study, it is likely that fractures produced by high velocity ballistic impacts follow a similar fracture cascade. Further research should extend to include higher velocity projectiles into samples with the soft tissue envelope preserved to confirm this likelihood.

Understanding this cascade will not only allow the clinician to better predict the severity of injury in lower velocity projectile trauma, but also, in higher velocity projectile trauma, allow the clinician to predict how the fracture fragments arose and what happened to them during the insult to better understand the dissipation of energy and optimal skeletal management.

**Figure 8.** The Previously Proposed Double Butterfly Fracture Mechanism

This study presents only the pre-impact kinetic energies rather than the energy transfer. While it can be noted that the energy transfer will be less than these reported, because no projectiles became embedded in the bone, the exact energy transfer was not determined. Pre-impact kinetic energy has been used as an indication of a projectile's potential to cause damage (18) and because the energy values we were studying were so low (0.013-5.35 J) we used these values to assess bone injury. However, energy transfer is more accurate at denoting the injury severity (19) and as such future studies should aim to use energy transfer as opposed to pre-impact kinetic energy. Furthermore, a better understanding of the dynamic response could be achieved with the applica-

tion of biosensors on the samples; further research should consider this modality.

To our knowledge, this is also the first study to utilize micro-CT to analyze fracture in ballistic skeletal injuries. This study has demonstrated the value of micro-CT as a powerful tool for imaging the bullet impact site. It was found to offer a more accurate measure of the resultant fracture morphology than the conventional basic fuchsin staining process, where artefactual damage from the dehydration, sawing and grinding process are likely and difficult to differentiate from injury incurred during impact (20).

Conclusions: Low velocity projectile impact fractures of the anterior mid-diaphysis of the femur follow a reproducible fracture cascade from indentation to the initiation of cone cracks followed by the development of radial cracks that propagate to form butterfly fractures. The development of radial fractures, along with subsurface tensional damage below the impact site, result in the extensive comminution observed. At much higher impact velocities shock wave effects may have made an additional contribution to the observed damage.

Acknowledgements

The authors wish to acknowledge Glynn Kieser for her editorial input.

Authors' Contribution

All authors made a significant contribution to all aspects of this research.

Financial Disclosure

No authors have financial interests related to the material in the manuscript.

Funding/Support

No funding was provided for this research. No sponsor was involved in this Research.

References

1. Dougherty PJ, Vaidya R, Silverton CD, Bartlett C, Najibi S. Joint and long-bone gunshot injuries. *J Bone Joint Surg Am.* 2009;**91**(4):980-97.
2. McGee AM, Qureshi AA, Porter KM. Review of the biomechanics and patterns of limb fractures. *Trauma.* 2004;**6**(1):29-40.
3. Hansen U, Zioupos P, Simpson R, Currey JD, Hynd D. The effect of strain rate on the mechanical properties of human cortical bone. *J Biomech Eng.* 2008;**130**(1):110-11.
4. Rockwood CA, Green DP, Bucholz RW. *Fractures in adults.* 7th ed: Lippincott Williams & Wilkins; 2010.
5. Huelke DF, Darling JH. Bone Fractures Produced by Bullets. *J Forensic Sci.* 1964;**9**(4):461-9.
6. Smith HW, Wheatley KK, Jr. Biomechanics of femur fractures secondary to gunshot wounds. *J Trauma.* 1984;**24**(11):970-7.
7. Chen Y, Miao Y, Xu C, Zhang G, Lei T, Tan Y. Wound ballistics of the pig mandibular angle: a preliminary finite element analysis and experimental study. *J Biomech.* 2010;**43**(6):1131-7.
8. Tang Z, Tu W, Zhang G, Chen Y, Lei T, Tan Y. Dynamic simulation and preliminary finite element analysis of gunshot wounds to the human mandible. *Injury.* 2012;**43**(5):660-5.
9. Wrightman G, Beard J, Allison R. An investigation into the behaviour of air rifle pellets in ballistic gel and their interaction with bone. *Forensic Sci Int.* 2010;**200**(1-3):41-9.
10. Kieser DC, Kanade S, Waddell NJ, Kieser JA, Theis JC, Swain MV. The deer femur: A morphological and biomechanical animal model of the human femur. 2013:[Epub ahead of print].
11. Huelke D, Buegge L, Harger J. Bone fractures produced by high velocity impacts. *Am J Anat.* 1967;**120**:123-31.
12. Huelke DF, Harger JH, Buege LJ, Dingman HG, Harger DR. An experimental study in bio-ballistics femoral fractures produced by projectiles. *J Biomech.* 1968;**1**(2):97-105.
13. Burr DB, Hooser M. Alterations to the en bloc basic fuchsin staining protocol for the demonstration of microdamage produced in vivo. *Bone.* 1995;**17**(4):431-3.
14. Knight CG, Swain Michael V, Chaudhri MM. Impact of small steel spheres on glass surfaces. *J Material Sci.* 1977;**12**(8):1573-86.
15. Ball A, McKenzie HW. On the low velocity impact behavior of glass plates. *J Phys IV.* 1994;**4**:783-8.
16. Harger JH, Huelke DF. Femoral fractures produced by projectiles-the effects of mass and diameter on target damage. *J Biomech.* 1970;**3**(5):487-93.
17. Sellier KG, Kneubuehl BP. *Wound ballistics, and the scientific background.* Amsterdam: Elsevier Science BV; 1994.
18. Churvis A. Ballistics of penetration. *SWAT.* 1983;**2**:34-8.
19. Adams DB. Wound ballistics: a review. *Mil Med.* 1982;**147**(10):831-5.
20. Lee TC, Mohsin S, Taylor D, Parkesh R, Gunnlaugsson T, O'Brien FJ, et al. Detecting microdamage in bone. *J Anat.* 2003;**203**(2):161-72.